Nonlinear Hall Resistivity in $YBa_2Cu_3O_{7-\delta}$ Films near the Vortex-Glass Transition

P. J. M. Wöltgens, C. Dekker,* and H. W. de Wijn
Faculty of Physics and Astronomy, and Debye Institute, Utrecht University, P.O. Box 80.000, 3508 TA Utrecht, The Netherlands
(Received 9 September 1993)

The Hall electric field E_y is observed to be a strongly nonlinear function of the current density J_x in the vicinity of the vortex-glass transition of $YBa_2Cu_3O_{7-\delta}$ films in a magnetic field. Much like the longitudinal electric field E_x, E_y appears to scale critically with J_x, with a Hall-related critical exponent $\lambda = 3.4 \pm 0.3$. Furthermore, the Hall resistivity $\rho_{xy} = E_y/J_x$ and the longitudinal resistivity $\rho_{xx} = E_x/J_x$ are found to obey $\rho_{xy} \propto \rho_{xx}^{2.0\pm0.2}$ over a wide range of current densities and temperatures. The results quantitatively verify recent theoretical predictions.

PACS numbers: 74.60.Ge, 73.50.Jt, 74.76.Bz

In this Letter, we report on the first observation of *nonlinear* Hall resistivity in $YBa_2Cu_3O_{7-\delta}$ films in the vicinity of the vortex-glass transition in a high magnetic field, i.e., the Hall electric field E_y is a nonlinear function of the driving longitudinal current density J_x. At the vortex-glass transition temperature T_g, $YBa_2Cu_3O_{7-\delta}$ films pass from a vortex liquid to a vortex glass state [1]. As it appears, the Hall resistivity becomes increasingly of nonlinear character upon approaching T_g from above, and turns entirely nonlinear below T_g.

Entering the nonlinear regime implies, as quite general arguments show [1], that the length scales on which the system is probed becomes of the order of the vortex-glass correlation length, which diverges at T_g. It therefore puts theories of the Hall effect relying on vortex dynamics to a particularly severe test. This, in fact, is the objective of this Letter. Contrary to the nonlinear Hall effect, the linear Hall effect, which is only observed at sufficient distance from the transition and at sufficiently low currents, has recently attracted considerable attention. The focus of the interest has been on the intriguing sign change that occurs upon cooling from the normal to the vortex liquid state [2–8]. Of particular relevance here furthermore is the finding by Luo *et al.* [9] that in the linear regime the Hall resistivity $\rho_{xy} = E_y/J_x$ as a function of the temperature follows a power-law dependence on the longitudinal resistivity $\rho_{xx} = E_x/J_x$.

Two theories are available for the Hall effect in superconductors in the nonlinear regime. First, inspired by the results of Luo *et al.* [9], Dorsey and Fisher (DF) [10] devised a critical scaling model, elaborating on the fact that the Hall effect in superconductors is an expression of the particle-hole asymmetry. In the vicinity of the vortex-glass phase transition [1], this asymmetry is assumed to scale with a power of the vortex-glass correlation length. The linear Hall resistivity then exhibits a critical scaling behavior, in consistency with experiment [9]. Furthermore, DF made an explicit prediction for the Hall effect, which may serve as an independent test of their theory: "The *nonlinear* Hall electric field E_y should exhibit universal scaling, and right at the transition should vanish with a universal power of the current density J_x."

An alternative, but not necessarily incompatible, approach has very recently been put forward by Vinokur, Geshkenbein, Feigel'man, and Blatter (VGFB) [11]. These authors consider the force balance for stationary moving vortices with disorder-dominated dynamics, such as provided by flux pinning. Their primary result is that scaling behavior of the Hall resistivity should be a general feature of the vortex state. An exact value of 2 is found for the exponent β in the scaling relation $\rho_{xy} \propto \rho_{xx}^{\beta}$. Furthermore, β is concluded to be universal, independent of parameters such as the temperature, the external magnetic field, and, of particular relevance here, the applied current density.

Below, we verify these theoretical predictions by Hall measurements in the nonlinear regime. The sample studied was a high-quality epitaxial $YBa_2Cu_3O_{7-\delta}$ film of 3000 Å thickness grown onto a (100) $SrTiO_3$ substrate by laser ablation. The c axis was perpendicular to the substrate. Photolithography and Ar-ion milling techniques were used to define a Hall bar with strip dimensions 150×20 μm^2. A gold layer was deposited onto the contact pads, and subsequently annealed, yielding a negligible contact resistance. In the absence of a magnetic field, the film exhibited zero resistance at 91.0 K. The E_y-J_x and E_x-J_x curves were taken by the use of an ac method employing a sine-wave current with an amplitude such as to cover the full range of E_x desired [12]. This ac method has the advantage over dc methods of averaging out any temperature rise over a period of the current to a steady-state temperature offset, thus eliminating distortion of the $E_{x,y}$-J_x curves as a result of current-induced heating. The temperature offset is estimated to be 0.2 K at most. With a driving ac current I_x of low frequency ($\sim$ 10 Hz) in the film plane, both the voltage $V_\parallel$ parallel and the voltage $V_\perp$ perpendicular to I_x were measured. With a digital oscilloscope the time traces of I_x, $V_\parallel$, and $V_\perp$ were simultaneously recorded, and averaged over typically 5000 periods to reduce noise and interference. The measurements were carried out in a magnetic field $\mathbf{H}$ of 3 T directed along the film c axis. Additional measure-

0031-9007/93/71(23)/3858(4)$06.00

ments at 2 T yielded essentially the same results. The data were collected with the magnetic field directed upwards and downwards under otherwise identical conditions. The Hall voltage V_y was subsequently equated to the antisymmetric part of $V_\perp$, i.e., $V_y = \frac{1}{2}(V_{\perp,\uparrow} - V_{\perp,\downarrow})$, where the subscripts $\uparrow$ and $\downarrow$ refer to field up and down, respectively. Similarly, we took $V_x = \frac{1}{2}(V_{\parallel,\uparrow} + V_{\parallel,\downarrow})$ for the longitudinal voltage, although $V_{\parallel,\uparrow}$ and $V_{\parallel,\downarrow}$ differed typically by less than 0.5%.

In Fig. 1 is presented a selected set of the measured E_y-J_x curves. These curves, separated by 1 K intervals, were collected from near the temperature at which the linear Hall effect changes its sign ($\approx$ 88 K) all the way down to 76 K, i.e., 4 K below the vortex-glass transition temperature $T_g = 79.9$ K. The noteworthy finding from Fig. 1 is that in this temperature range the Hall resistivity changes from being essentially linear to completely nonlinear. At 88 K, for instance, we find $E_y \propto J_x^{1.0}$, whereas at 76 K, $E_y \propto J_x^{5.6}$. Figure 2 shows, in a log-log plot, a set of E_y-J_x curves along with the corresponding set of E_x-J_x curves. The longitudinal electric field E_x complies with the by now well-established critical behavior [12]: The E_x-J_x curves show a crossover from Ohm's law at high temperatures via a power-law dependence at T_g to exponential behavior at low temperatures. At high current densities and electric fields (> 10 V/m), however, minor departures towards Ohmic behavior show up. These have been observed before [13], and presumably are related to approach of the flux-flow regime. Below, we will, therefore, distinguish between the data at "low" and "high" current densities. At T_g, we find $E_x \propto J_x^{3.1}$ at low current densities.

The Hall electric field E_y behaves in a way quite analogous to E_x, as is observed from Fig. 2. Upon cooling to T_g from above, the E_y-J_x curves exhibit a gradual crossover from an Ohmic to a power-law dependence. At T_g, we have $E_y \propto J_x^{4.4}$. This, in fact, constitutes a very direct verification of the predictions by DF. In the crossover regime above T_g, E_y vs J_x changes from a linear to a power-law dependence upon raising the current. Closer inspection reveals that the current density J_x where nonlinearity of E_y sets in is of the order of the J_x above which E_x becomes nonlinear, and furthermore has the same temperature dependence. At temperatures below T_g, the dependence of E_y on J_x becomes progressively more nonlinear. Below T_g, E_y could only be measured over a limited range, so a possible negative curvature in E_y vs J_x, or for that matter a genuine exponential dependence, could not be discerned unambiguously.

We now turn to a detailed critical-scaling analysis according to DF. The idea of critical scaling near a continuous phase transition is ultimately based on the concept of a diverging correlation length. In the present context, the relevant correlation length is the vortex-glass correlation length ξ [1]. At T_g, it diverges according to

$$\xi \propto 1/|T - T_g|^\nu , \tag{1}$$

in which ν is the static critical exponent. DF postulate that, near the vortex-glass transition, the particle-hole asymmetry of the superconducting wave function scales as $\xi^{-\lambda}$, where λ is a new universal critical exponent. For the nonlinear Hall electric field E_y they then derive, for three-dimensional systems, the scaling relation

$$E_y = \xi^{1-z-\lambda} J_x \mathcal{G}_\pm(J_x \xi^2/T) . \tag{2}$$

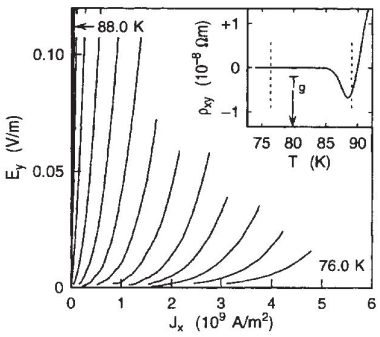

FIG. 1. Set of E_y-J_x Hall curves at 3 T for temperatures between 76 and 88 K. Consecutive E_y-J_x curves differ by temperature intervals of 1 K. The inset shows the linear Hall resistivity vs the temperature as measured at $J_x = 5 \times 10^6$ A/m^2 and 3 T. The linear Hall effect changes sign around 90 K, and vanishes below about 83 K. The dashed lines delimit the temperature range in which the E_y-J_x curves were measured.

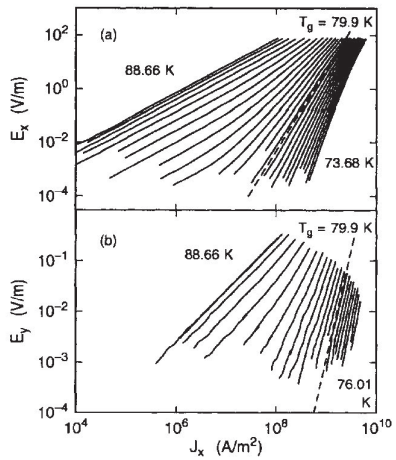

FIG. 2. Log-log plot of (a) the longitudinal electric field E_x and (b) the Hall electric field E_y vs the current density J_x at various temperatures and 3 T. Consecutive curves differ by temperature intervals of approximately 0.60 K. The dashed lines represent the power-law behavior at T_g (for E_x at "low" currents).

Here, $\mathcal{G}_\pm$ is the scaling function, which differs for temperatures above (+) and below (−) T_g, and z is the dynamical critical exponent. For comparison, the scaling relation for the longitudinal electric field E_x reads [1]

$$E_x = \xi^{1-z} J_x \mathcal{F}_\pm(J_x \xi^2/T) \ , \qquad (3)$$

with $\mathcal{F}_\pm$ the scaling function above (+) and below (−) T_g. Note that Eq. (2) differs from Eq. (3) mainly by the factor $\xi^{-\lambda}$.

In preparation of verifying DF critical scaling of the Hall voltage, we have first scaled all E_x-J_x data (cf. Fig. 2) with the purpose to determine T_g, z, and ν. Here, use is made of Eq. (3) in conjunction with Eq. (1) to eliminate ξ. Scaling of E_x implies that all data, when plotted in a single plot of $E_x/J_x|T-T_g|^{\nu(z-1)}$ vs $J_x/T|T-T_g|^{2\nu}$, fall onto a single curve, if at least the proper values for T_g, z, and ν are inserted. The resulting curve then represents the scaling function $\mathcal{F}_\pm$ itself. We again differentiate between the data sets at "low" and "high" currents. The optimum scaling collapse of all available data at low currents was accomplished for $T_g = 79.9 \pm 0.1$ K, $z = 5.2 \pm 0.2$, and $\nu = 1.75 \pm 0.10$. These results for z and ν are consistent with previous reports [12,14]. Because the low-current data are best suited to locate the transition, and T_g is insensitive to the current, we adopt the T_g so obtained throughout. Optimum scaling collapse for the high-current data, which is shown in Fig. 3(a), was then achieved for the effective exponents $z = 4.4 \pm 0.2$ and $\nu = 1.75 \pm 0.10$.

A principal result of the present work is that the nonlinear Hall data obey the predicted scaling behavior according to Eq. (2). To accomplish the collapse of E_y on a universal curve, we inserted the values for T_g, z, and ν arrived at in the scaling of E_x, so we were left with adjustment of the single parameter λ. For z and ν the high-current values were adopted, because the Hall data were collected in this regime. An excellent critical scaling collapse is then achieved for $\lambda = 3.4 \pm 0.3$, which is shown in Fig. 3(b). This collapse provides strong support for the DF theory. It is useful to consider the limiting case of T_g, which of course is contained in the scaling analysis, but for which the scaling function has a particularly simple form. At T_g, the Hall electric field should exhibit a pure power-law dependence, i.e., $E_y \propto J_x^{(z+\lambda+1)/2}$. The experimental exponent, i.e., the slope of E_y vs J_x in Fig. 3(b), amounts to 4.4, which indeed equals the value $(z + \lambda + 1)/2 = 4.4 \pm 0.3$ from the DF scaling analysis [15].

We next turn to examining the validity of the VGFB theory by considering ρ_{xy} in relation to ρ_{xx}. To this end, we first plot, for a given temperature, *all* data for ρ_{xy} [cf. Fig. 2(b)] as a function of the corresponding data for ρ_{xx} [cf. Fig. 2(a)], with the current density as running variable. Subsequently, we combine the ρ_{xy} vs ρ_{xx} plots so constructed in a single log-log graph, which is displayed in Fig. 4. With regard to the current dependencies of ρ_{xy} and ρ_{xx}, the important finding then is that these form straight lines for all temperatures considered, i.e., ρ_{xy} depends on ρ_{xx} according to $\rho_{xy} \propto \rho_{xx}^{\beta_J}$ all the way into the nonlinear regime. The exponent β_J, in which the subscript reminds one of the current being the running variable, is given in the inset of Fig. 4, and is seen to amount to 2.0 ± 0.2, and to drop slightly above 85 K. Equally remarkable is that above T_g these straight lines, when combined in Fig. 4, line up to form a single curve, except below T_g. This implies that also for the temperature dependences of ρ_{xy} and ρ_{xx} a quadratic power law is established ($\beta_T \approx 2$). It is noteworthy that this

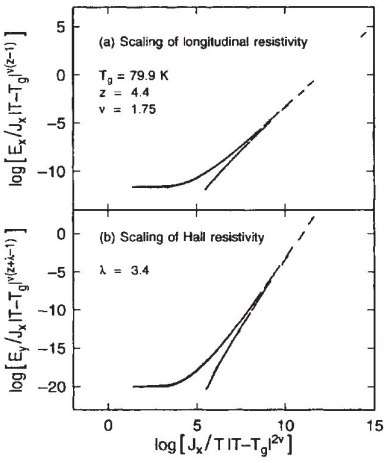

FIG. 3. Critical scaling collapse of over 100 isotherms between 76 and 86 K at 3 T for (a) E_x and (b) E_y.

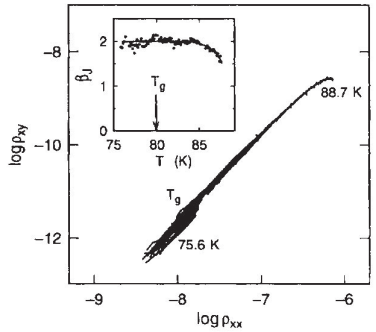

FIG. 4. Log-log plot of the Hall resistivity ρ_{xy} vs the longitudinal resistivity ρ_{xx} at 3 T. Both ρ_{xy} and ρ_{xx} are in units Ω m. The curve is built up from over 100 isotherms, with J_x as running variable. These isotherms cover only part of the curve, as indicated by the labels. The inset shows the exponent β_J vs the temperature, demonstrating that Eq. (4) holds over a large range of temperatures.

quadratic dependence of ρ_{xy} (ρ_{xx}) is seen to hold over at least 3 decades in ρ_{xy}. Summing up the findings related to Fig. 4, we conclude that both the current and temperature dependencies of ρ_{xy} and ρ_{xx} obey, over a wide range, the scaling relation

$$\rho_{xy}(J_x, T) = A[\rho_{xx}(J_x, T)]^{2.0\pm0.2} , \quad (4)$$

where A is a proportionality constant independent of J_x [16]. This quantitatively confirms the predictions of the VGFB model.

Finally, we compare the results derived with the DF and VGFB theories. These theories self-evidently are of entirely different nature. Critical phenomena as such, which are the basis of the DF theory, are not treated by the VGFB force-balance approach. From Eqs. (2) and (3) it is straightforward to derive that $\rho_{xy} = \rho_{xx}^{\beta}\mathcal{H}_{\pm}$, in which $\beta = (z + \lambda - 1)/(z - 1)$ and $\mathcal{H}_{\pm} = \mathcal{F}_{\pm}/\mathcal{G}_{\pm}^{\beta}$. In the limit of the linear regime as well as at T_g, $\mathcal{H}_{\pm} = 1$ exactly. Inspection of the data in Fig. 2 furthermore shows that $\mathcal{H}_{\pm} \approx 1$ holds throughout. Substituting the exponents arrived at from the DF critical scaling, we find the result $\beta = 2.0 \pm 0.2$. (The "high" current z should be used, as it refers best to the current regime where λ was obtained.) The fact that the β predicted by the the VGFB theory is retrieved from the DF critical scaling analysis leads to the conclusion that the DF and VGFB theories are mutually compatible in the sense that the specific combination of critical exponents $(z + \lambda - 1)/(z - 1)$ indeed appears to equal 2 within the errors.

In summary, we have measured the nonlinear Hall resistivity in a $YBa_2Cu_3O_{7-\delta}$ film near the vortex-glass transition. Critical scaling behavior of the nonlinear Hall voltage according to the DF model [10] has been verified. Over an extended range of temperatures and current densities, the data furthermore exhibit a quadratic dependence of the Hall resistivity on the longitudinal resistivity, as predicted by VGFB [11].

We thank W. J. Gallagher and W. Eidelloth of IBM Yorktown Heights for mask design and film growth. We furthermore acknowledge discussions with G. Blatter, A. T. Dorsey, V. B. Geshkenbein, P. Tiesinga, and V. M. Vinokur. The work was in part supported by the Netherlands Foundation "Fundamenteel Onderzoek der Materie (FOM)" and the "Nederlandse Organisatie voor Wetenschappelijk Onderzoek (NWO)."

* Present address: Department of Applied Physics, Delft University of Technology, Lorentzweg 1, 2628 CJ Delft, The Netherlands.

[1] D. S. Fisher, M. P. A. Fisher, and D. A. Huse, Phys. Rev. B **43**, 130 (1991).

[2] M. Galffy and E. Zirngiebl, Solid State Commun. **68**, 929 (1988).

[3] Y. Iye, S. Nakamura, and T. Tamegai, Physica (Amsterdam) **159C**, 616 (1989).

[4] S. J. Hagen, C. J. Lobb, R. L. Greene, and M. Eddy, Phys. Rev. B **43**, 6246 (1991); **47**, 1064 (1993).

[5] T. R. Chien, T. W. Jing, N. P. Ong, and Z. Z. Wang, Phys. Rev. Lett. **66**, 3075 (1991).

[6] Z. D. Wang and C. S. Ting, Phys. Rev. Lett. **67**, 3618 (1991); Phys. Rev. B **46**, 284 (1992).

[7] A. T. Dorsey, Phys. Rev. B **46**, 8376 (1992).

[8] N. B. Kopnin, B. I. Ivlev, and V. A. Kalatsky, Pis'ma Zh. Eksp. Teor. Fiz. **55**, 717 (1992) [JETP Lett. **55**, 750 (1992)].

[9] J. Luo, T. P. Orlando, J. M. Graybeal, X. D. Wu, and R. Muenchausen, Phys. Rev. Lett. **68**, 690 (1992).

[10] A. T. Dorsey and M. P. A. Fisher, Phys. Rev. Lett. **68**, 694 (1992).

[11] V. M. Vinokur, V. B. Geshkenbein, M. V. Feigel'man, and G. Blatter, Phys. Rev. Lett. **71**, 1242 (1993).

[12] R. H. Koch, V. Foglietti, W. J. Gallagher, G. Koren, A. Gupta, and M. P. A. Fisher, Phys. Rev. Lett. **63**, 1511 (1989); R. H. Koch, V. Foglietti, and M. P. A. Fisher *ibid.* **64**, 2586 (1990).

[13] C. Dekker, W. Eidelloth, and R. H. Koch, Phys. Rev. Lett. **68**, 3347 (1992).

[14] C. Dekker, P. J. M. Wöltgens, R. H. Koch, B. W. Hussey, and A. Gupta, Phys. Rev. Lett. **69**, 2717 (1992).

[15] A second limiting case is the linear regime, occurring at low current densities and high temperatures. Here, Eqs. (2) and (3) reduce to $\rho_{xy} \propto (T - T_g)^{\nu(z+\lambda-1)}$ and $\rho_{xx} \propto (T - T_g)^{\nu(z-1)}$. Accordingly, the power law $\rho_{xy} \propto \rho_{xx}^{\beta_T}$ with $\beta = (z + \lambda - 1)/(z - 1)$ holds exactly. From data such as the ones in Fig. 2, we derive for the linear regime $\nu(z + \lambda - 1) = 12 \pm 1$ and $\nu(z - 1) = 7.3 \pm 0.3$, whence $\beta_T = 1.7 \pm 0.3$. This agrees with the slightly diminished β_J above 85 K (cf. Fig. 4), the result $\beta_T = 1.7 \pm 0.2$ extracted from the linear Hall resistivity by Luo *et al.* [9], and similar results from previous experiments [J. P. Rice, N. Rigakis, D. M. Ginsberg, and J. M. Mochel, Phys. Rev. B **46**, 11 050 (1992); R. C. Budhani, S. H. Liou, and Z. X. Cai, Phys. Rev. Lett. **71**, 621 (1993); A. V. Samoilov *ibid.* **71**, 617 (1993)].

[16] Comparison of our data at 2 and 3 T suggest that A decreases with an external magnetic field, in consistency with VGFB.